10.1149/1.3613182 © The Electrochemical Society

Si Nanocrystals Embedded in SiO_2 Produced by Reactive Sputtering for Light Emission

A. E. P. Mattos, G. Sombrio, P. L. Franzen, M. B. Pereira and H. Boudinov

Instituto de Física, UFRGS, Porto Alegre, RS, 91501-970, Brazil

In the present work, we confectioned light emitting SiO_x ($x<2$) samples using reactive sputtering. By controlling the oxygen concentration in the deposition chamber (range from 0.5% up to 10), an excess of silicon was created in the formed silicon oxide films. Only after a thermal annealing (temperatures from 1050ºC to 1100ºC), the samples showed the photoluminescence (PL) effect. Silicon nanocrystals formed during the thermal annealing were the responsible for the observed PL signal when excited with the 488nm line of argon laser. We also performed thermal annealing at 450ºC, using forming gas ambient to passivate the silicon nanocrystals interface. The result was a significant improvement in PL signal. Furthermore, the Rutherford Backscattering Spectrometry experiment showed that the deposition time is an important parameter to create the silicon excess and achieve light emission.

Introduction

Bulk silicon has an indirect band gap and for this reason it was considered unsuitable for optoelectronic applications. Nevertheless, it was discovered that silicon nanocrystals embedded in an isolator matrix can be optically active, due to quantum confinement effects (1). This characteristic of silicon has stimulated new research in the area of silicon-based optoelectronics. Recent studies discuss the photoluminescence (PL) and electroluminescence (EL) proprieties of silicon nanocrystals (Si-nc) made by different techniques: ion implantation (2-4), plasma-enhanced chemical vapor deposition (PECVD) (5, 6) and magnetron sputtering (7). All these techniques are used to create silicon excess inside the isolator. Ion implantation can only create one region of silicon excess due to the implantation parameters (8), while PECVD and sputtering were used to make superlattices by alternating isolator and silicon layers.

To segregate the silicon excess into nanocrystals, thermal annealing is required. It is known that several parameters can contribute to light emission from silicon nanocrystals (9). Two important characteristics of the PL signal are the number and the size of Si-nc. Additionally, in the interface between silicon and the isolator, defects and impurities contribute to nonradiative transitions. However, the shape of PL signal spectra is correlated with the nanocrystals size distribution. Big grains will contribute for longer wavelengths and the small ones will contribute to shorter wavelengths (10).

In this work, we present Si-nc made by reactive sputtering using a mixture of argon and oxygen, where the partial pressures of the gases are controlled in the deposition chamber. We are able to control the target sputtering rate by monitoring the total pressure as well as the oxidation of the sputtered material by changing the partial pressure of

oxygen. Using reactive sputtering, we create films that have silicon excess, uniformly distributed throughout the oxide matrix. Since sputtering is a deposition technique widely used in microelectronics industry and is performed at room temperature, the use of photoluminescent and electroluminescent thin films based on silicon becomes economically attractive.

Experiment

Several samples were prepared to determine the best deposition parameters. The deposition was performed in a Perkin-Elmer 4450 sputtering chamber, using a silicon target. Previously cleaned <100> silicon wafer were used as substrate. After the deposition, the samples were annealed to segregate the silicon excess into silicon nanocrystals. Using a conventional horizontal furnace and an argon flow, different regimes of time and temperature were tested. The annealing was performed in a temperature range from 500°C to 1200°C for times that vary from 5min to 60min. Furthermore, the annealing process with forming gas (FG - 90% of N_2 and 10% of H_2) at 450°C for 30 minutes was also tested.

The photoluminescence measurements were realized at room temperature using the 488nm (2.54eV) line of an Ar-ion laser (Melles Griot 35 IMA 410-120) as excitation source. The laser power was controlled with a continuously variable ND filter. The photoemission was analyzed with the aid of a gridded monochromator (Acton SP2300 with a 300 grids/mm). To avoid interference between the pumping signal and the spectra, a low-pass filter (cutoff at 540 nm) was placed at the entrance of the monochromator. The signal was collected with a CCD (PIXIS 256) camera connected to a PC.

Rutherford Backscattering Spectrometry (RBS) was used to assess the films stoichiometry. A beam of 1MeV He^+ ions, provided by a Tandetron accelerator, was directed to the samples. The backscattered particles were detected at 10º with respect to incident beam. Moreover, a Spectral Ellipsometer SOPRA GES-5E was used to obtain the thickness of the samples (spectral range from 250 to 850nm and angle of incidence of 75°).The Ellipsometer's analysis-modeling software (Winelli 2.2.0.7) uses a set of silicon oxide refractive index values from literature to calculate the film thickness. The R^2 value (11) from the fitting between the assumed model and the experimental data provides us an idea of the quality of the deposited film.

Table I synthesizes the deposition parameters of our samples. All depositions were performed using the same RF power (1kW). We varied the O_2 concentration in the deposition chamber from 0.5% to 10%, while total pressure was maintained constant. Sample G did not form an oxide film, therefore its thickness value is missing in Table I.

TABLE I. The samples deposition parameters.

Sample	O_2 Concentration	Total Pressure	Deposition Time	Thickness (nm)	PL signal
A	10%	10mtorr	20min	94	NO
B	5%	10mtorr	20min	126	NO
C	3%	10mtorr	20min	120	NO
D	2%	10mtorr	20min	135	NO
E	1%	10mtorr	10min	475	YES
F	1%	10mtorr	20min	890	YES
G	0,5%	10mtorr	20min	-	NO
H (rotating)	1%	10mtorr	180min	740	YES

Results

The ellipsometry results showed that the samples without PL signal can be assumed as perfect thermal silicon oxide – the fitting used in this model was very good ($R^2 \approx 1$). On the other hand, similar assumption cannot be made for the samples with PL signal – it was not possible to obtain a good fitting using the thermal silicon oxide model. As presented in Table I, only the samples E, F and H showed photoluminescence signal, as a result of the silicon excess in those samples.

Figure 1 shows the photoluminescence spectra of sample F, after annealing at 1050ºC for 30 minutes in argon flow, for several excitation powers.

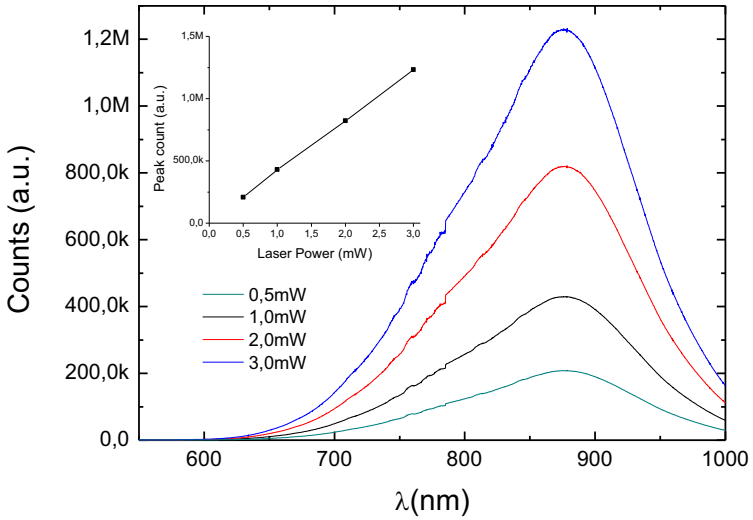

Figure 1 Room temperature PL spectra of sample F at different laser powers that were used. The inset shows the linear behavior of the counts as a function of the laser power

Increasing the excitation power, the only change that could be observed was a rising in the PL intensity. There was no significant shift in the peak position and the luminescence linear behavior (inset graph) indicates that the saturation regime was not reached for sample F. The other samples that showed PL effect did not reach the saturation regime too in this power range.

Figure 2 shows the PL spectra for samples F and H. Both samples were measured after annealing at 1050ºC in argon flow. These two samples were fabricated using the same oxygen concentration. Sample F was deposited with sample holder fixed and sample H was deposited with the sample holder rotating. The deposition time for sample H was calculated to reach more or less the same film thickness as sample F. Sample F has the PL peak at 865nm and sample F has at 750nm and the PL intensity is seven times higher in sample F than in sample H.

The difference in the PL behaviors seen at figure 2 can be clarified by RBS measurements. Using the technique is possible to quantify the silicon excess and estimate the films stoichiometry. In both experiments, the same geometry and total ion dose were

used in RBS measurements for comparison (see Figure 3). Table II shows the relative atomic concentrations in samples F an H, which were calculated from RBS spectra (12).

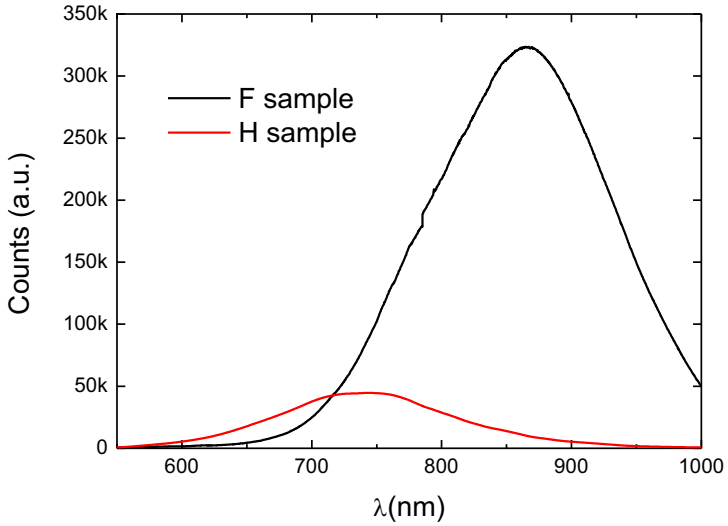

Figure 2. PL spectra from samples F and H after thermal annealing at 1050°C (argon atmosphere for 30 minutes). It was used a laser with 1mW power in both measurements. The main difference between samples F and H is that the first was made with the sample holder static, the second was done with the sample holder rotating.

TABLE II. Relative elemental amounts in the samples.

Sample	O_2 (%)	Si (%)
F	62 ±3	38 ±3
H	70 ±4	30 ±4

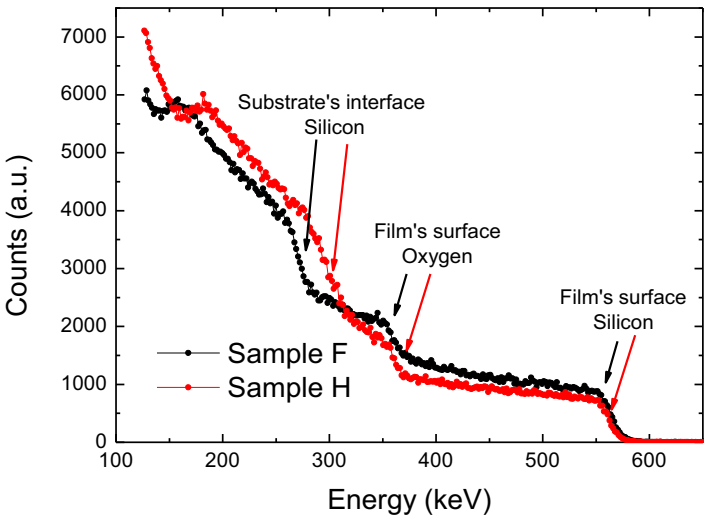

Figure 3. RBS spectra of samples F and H. The arrows indicate the surface of the oxide film, the oxygen in the film and the contribution from silicon substrate. These spectra were performed without channeling.

Sample H presents more oxygen than sample F because when the sample holder is rotating, the substrate only stays a few moments under the target at every turn. In the remaining time the Si deposited over the substrate is exposed to oxygen. Consequently, a larger fraction of silicon excess in sample H was oxidized, resulting in smaller and fewer Si-nc than in sample F. So, the spectrum of sample H in figure 2 is less intense and blue shifted due to the smaller average size of the Si-nc in sample H.

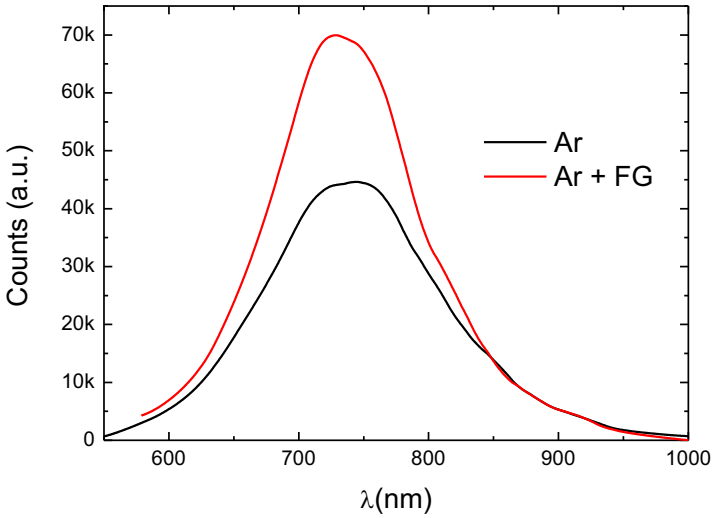

Figure 4. In black, PL spectra measured from sample H after thermal annealing at 1050ºC in argon atmosphere. In red, the same sample after a second thermal annealing at 450ºC for 30 minutes, in forming gas ambient.

The interface between the nanocrystals and the silicon oxide contains dangling bonds and defects that are responsible for nonradiative transitions. During the annealing in forming gas, H_2 reduces the number of states in the Si-nc surface and enhances the probability of photon emission. Figure 4 shows this effect. The PL signal of sample H exhibits a significant improvement in intensity after FG treatment. On other hand, it did not change the shape, because of the low temperature (450°C) which was used for this passivation.

Conclusions

The samples whose ellipsometry results exhibited similar behavior to thermal oxides did not have any photoluminescence signal. Only those samples deposited with 1% of O_2 resulted in films with PL. At high concentrations of oxygen, the silicon excess was not enough to create Si-nc. In concentrations lower than 1%, it is not possible to observe the typical oxide layer on the silicon subtract. We also distinguished a difference in PL signals from samples F and H. While the PL peak of the sample F is at 865nm, the PL peak from sample H is located at 750nm. This fact shows a difference in size distribution and the number of silicon nanocrystals between these two samples. The highest intensity and longer wave PL peak position of the PL from sample F is probably because of the larger number and larger average size of silicon nanocrystals than in sample H. The annealing temperature plays an important role in the formation of the nanocrystals light emitters. In temperatures under 1050ºC, no sample presented PL emission (not shown

here). The H_2 acts as a passivator of the interface states, which are nonradioactive recombination centers. That explains the PL signal improvement after annealing with forming gas.

Acknowledgments

The authors acknowledge financial support from CNPq and INCT NAMITEC

References

1. V. Vinciguerra, G. Franzo, F. Priolo, F. Iacona and C. Spinella, *J. Appl. Phys.*, **87**, 11 (2000).
2. U. S. Sias, M. Behar, H. Boudinov et all, *J. Appl. Phys.*, **98**, 3 (2005).
3. U. S. Sias, M. Behar, H. Boudinov et all, *J. Appl. Phys.*, **102**, 4 (2007).
4. U. S. Sias, M. Behar and E. C. Moreira, *Beam Interaction with Materials & Atoms*, **266** (2008).
5. L. Gong-Ru, L. Chun-Jung, L. Chi-Kuan et all, *J. Appl. Phys.*, **97**, 9 (2005).
6. A. Irrera, F. Iacona, I. Crupi et all, *Nanotechnology*, **17** (2006).
7. K. J. Kim, D. W. Moon, S. Hong et all, *Thin Solid Films*, **478** (2005).
8. U. S. Sias, E. C. Moreira, E. Ribeiro et all, *J. Appl. Phys.*, **95**, 9 (2004).
9. L. Pavesi, C. Mazzoleni, G. Franzo and F. Priolo, *Nature*, **408**, 6811 (2000)
10. Iacona, F; Franzo, G; Spinella, C, *J. Appl. Phys.*, **87**, 3 (2000).
11. P. A. Soave, R. A. F. Dau, M. R. Becker, M. B. Pereira and F. Horowitz, *Opt. Eng.*, **48**, 1246031 (2009).
12. Laboratory of Nuclear Analytic Methods, Rutherford Backscattering Spectrometry. Available in: < http://neutron.ujf.cas.cz/vdg/methods_rbs.html >.